INFLUENCE OF OPERATIONAL GEOMETRY CHANGES ON TURBINE ACOUSTICS

S. Bauinger, S. Zerobin, A. Marn, E. Göttlich, F. Heitmeir

Institute for Thermal Turbomachinery and Machine Dynamics,
Graz University of Technology
Inffeldgasse 25A, 8010 Graz –Austria

ABSTRACT

Due to the fact that noise emitted by aero engines became a very important issue especially during the last few years, acoustic measurements were carried out downstream of the low-pressure turbine in a two-stage two-spool test turbine. The aim of these analyses was to determine the influence of small geometry changes in the flow path of the rig under engine-relevant conditions, which usually occur during the operation of an engine. These geometry changes include steps in the flow path and different rotor tip gaps, both generated by a non-uniform warming of different parts of the engine. In order to evaluate the noise emissions, the outflow duct downstream of the second rotor was instrumented with an acoustic measurement section, which uses a circumferentially traversable microphone array located at the outer endwall. The acoustic field is characterized by azimuthal modes gained by traversing the microphone array over 360 degrees. Therefore, the spectra and emitted sound pressure levels are compared regarding different geometry changes.

NOMENCLATURE

A_{mn}	radial amplitude
B	number of blades
c	speed of sound
c_{ax}	axial chord length
f	frequency
f_{mn}	modal shape factor
h	duct height; harmonic index
k	integer index; wave number
k_{mn}	axial wave number
m	circumferential mode
n	radial mode
p	pressure
r	radius
Re	Reynolds number
t	time
V	number of vanes
p_t	total pressure
N_φ	number of circumf. meas. positions
x	axial coordinate
α	constant factor defining the opening angle of the horn
α_{mn}	complex cut-on factor
ρ	density
σ_{mn}	Bessel coefficient
ω	angular frequency
φ	circumferential position

Abbreviations

BPF	Blade Passing Frequency
HP	High Pressure
LP	Low Pressure
SPL	Sound Pressure Level
TMTF	Turning Mid Turbine Frame
TTTF	Transonic Test Turbine Facility
BFS	Backward Facing Step
FFS	Forward Facing Step
AMA	Azimuthal Mode Analysis

INTRODUCTION

In the last few years, the Institute of Thermal Turbomachinery and Machine Dynamics (TTM) has put a lot of effort into the experimental investigation of turbine acoustics and the development of appropriate post processing tools. Due to increasing bypass ratios and new technologies like geared turbofans, jet and fan noise have become less dominant in a modern turbofan engine. Therefore, the contribution of the noise emitted by the turbine gets more relevant and a better understanding of all the influencing variables becomes inevitable. Moser et al. (2009) were the first ones at TTM who carried out acoustic measurements in a 1.5 half-stage turbine using a microphone array. While Santner et al. (2011) regarded the aerodynamics of a two-stage two-spool turbine rig, where the LP and the HP stage are connected via an S-shaped duct, Faustmann et al. (2013) performed acoustic measurements downstream of the LP stage. In a further work, Faustmann et al. (2014) compared two different ducts with respect to noise emissions. The currently presented measurements were carried out in the same test rig, but focusing on operational geometry changes, which occur during the run-up and shut-down of an engine. By operational geometry changes, one can on the one hand understand backward and forward facing steps in the flow channel, which are generated by shifting the S-shaped duct and the parts further downstream in horizontal direction while the HP rotor and its casing were kept in the same position. In a real engine, these steps occur due to an ovalisation of non-segmented transition ducts, which are predominantly part of smaller engines. A non-uniform warming of the duct during operation, especially during run-up, causes this duct ovalisation. On the other hand, the influence of a tighter rotor tip gap on the noise emissions was investigated. The rotor tip clearance also changes during operation of an engine because of temperature changes and unequal thermal expansion of the rotor itself and the rotor casing. It is therefore also of big importance to gain knowledge of the modified behavior of the noise emissions due to tip gap changes especially during run-up. During this phase, the biggest changes of gap size take place. Kameier and Neise (1997) carried out experimental investigations on the influence of different rotor tip clearance sizes on the acoustic performance of an axial fan; however, as discussed in Bräunling (2009), the mechanisms of noise generation are very similar to those in a turbine stage. The only significant difference is that the turbine spectra are dominated by tonal and not broadband noise. In their publication, Kameier and Neise showed among other things a difference in broadband level depending on the tip clearance size. The level increased by several dB with increasing tip gap. Similar findings were made by Zhu and Carolus (2013), who carried out numerical as well as experimental investigations for an axial fan. Additionally, they showed that the amplitudes at the blade passing frequency and its harmonics are the same for different tip gaps at the design point of the rotor. To the authors' knowledge, several studies on tip gap variations in axial fans have been carried out up to now, but little literature exists for turbine rotors. Also, no experiments dealing with the influence of steps in the flow path on turbine acoustics could be found, which makes the current investigations even more important.

EXPERIMENTAL SETUP

All the measurements were carried out in the Transonic Test Turbine Facility (TTTF) at the Institute for Thermal Turbomachinery and Machine Dynamics at Graz University of Technology. This facility is a continuously operating two-stage two-spool turbine test rig, which is used in open circuit operation mode. It consists of a transonic HP stage and a LP stage with counter-rotating rotor. The rig is driven by pressurized air delivered by a 3 MW electrically driven compressor station. The power output of the HP rotor is used to drive a three-stage radial brake compressor, which delivers additional air. The two mass flows, one originating from the compressor station and one from the brake compressor, are merged in a complex system consisting of a mixer and a tandem cascade at the inlet of a mixing chamber. Therefore the overall mass flow can be increased.

The inlet temperature of the rig can be adjusted between 40°C and 185°C by cooling the air coming from the compressor station. However, the mass flow, which is delivered by the brake compressor, cannot be cooled. With the two air flows an overall mass flow of up to 22 kg/s can be achieved. Due to the design of the mixing chamber, the inlet pressure is limited to 4.5 bar absolute. The maximum shaft speeds are limited to 11550 rpm for the HP rotor and 4500 rpm for the LP rotor respectively. For the absorption of the LP turbine power a waterbrake with a maximum coupling power of 700 kW is used. The current test setup consists of a single-stage unshrouded transonic HP turbine and a shrouded counter-rotating LP rotor. Those two are connected by an S-shaped turning mid turbine frame (TMTF). That means the air enters the rig through the mixing chamber, flows through the HP turbine and is then turned in negative direction relative to the rotation of the HP rotor by the 16 struts of the TMTF. Downstream of the duct the air enters the LP rotor at a larger diameter. The flow leaves the test section through support struts and a diffuser in order to recover partially pressure of the air before entering the exhaust casing. Figure 1 shows a schematic cross-section of the test rig including the acoustic measurement section, which is located downstream of the LP rotor.

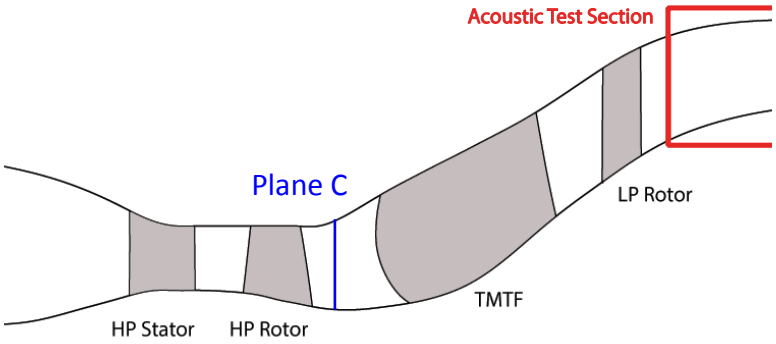

Figure 1: Schematic cross-section of transonic test turbine facility (TTTF)

The most important blading parameters and operating conditions are presented in Table 1.

Table 1: Blading parameters and operating conditions

Blading Parameters and Operating conditions						
	HP vane	HP blade	Struts	LP blade		
Vane/ blade no.	24	36	16	72	BPF_{HP} $[kHz]$	6.69
h/c_{ax}	1.15	1.37	0.53	2.94	BPF_{LP} $[kHz]$	4.26
Re(10^6)	2.38	1.1	1.86	0.46	Stage p_t ratio HPT/ LPT	3/ 1.3
Tip gap	unshrouded	-	-	-	Power [MW] HPT/ LPT	1.44/ 0.3

Test setups

In order to generate a backward respectively a forward facing step in the flow path, the TMTF and the whole aft rig were shifted laterally 2.5% of the channel height in plane C. The term aft rig describes in this case all the parts downstream of the HP stage. By shifting also the aft rig, steps were avoided downstream of the duct. HP stator, HP rotor, their casings and of course also the liner ring of the HP rotor with the abradable coating were kept in the same position. Figure 2 represents the described steps in the flow path and should reveal the geometrical setup of these investigations.

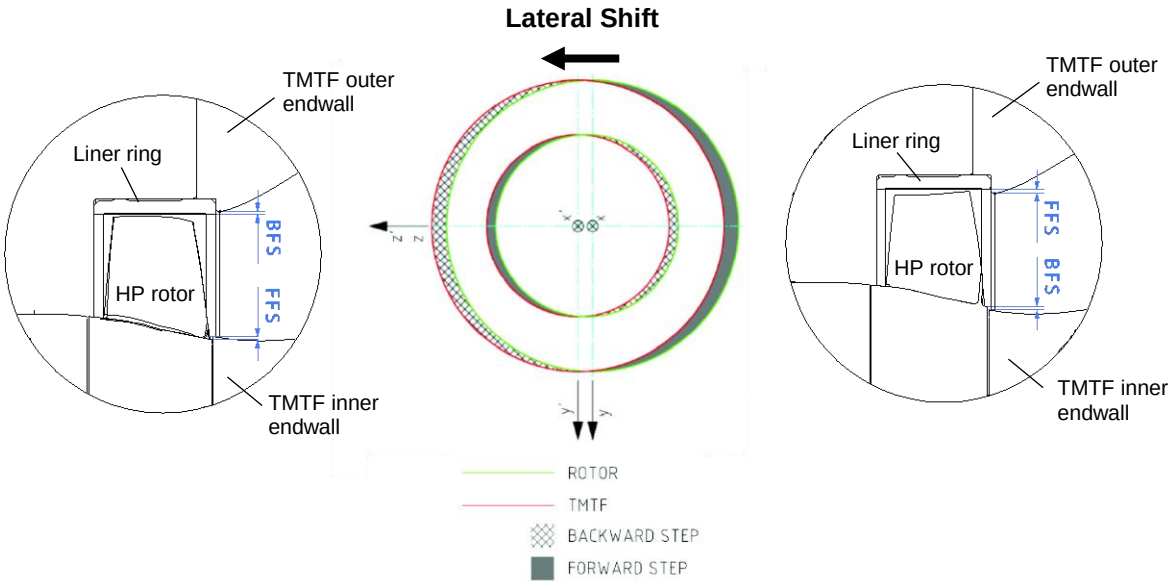

Figure 2: Details of backward and forward facing steps; right scheme shows the right half of the concerned test section, left scheme the left half

When looking against the flow direction, a forward facing step (FFS) between the duct outer casing and the rub ring was generated at the right half of the test rig while a backward facing step (BFS) is formed at the left half. Between the disk and the duct inner casing the opposite happens: there is a backward facing step at the right half and a forward facing step at the left half. As already mentioned, these steps are generated due to an ovalisation of the duct during the run-up of an engine. In the following the influence of the steps on turbine acoustics is experimentally investigated.
The second effect, which occurs during the operation of an engine, are changing tip clearances between the rotor blades and the outer casing. In the test rig, these different tip clearance sizes were not realized by parts with different thermal expansion but by using liner rings with different inner diameters.

Measurement technique and data acquisition

A detailed description of the microphone array, which is used for the acoustic measurement, is presented in Faustmann et al. (2014). The microphone array was designed by the Department of Engine Acoustics of the DLR Institute of Propulsion Technology according to the guidelines described in Tapken and Enghardt (2006). The challenge was to optimize the microphone arrangement with regard to the limited installation space and the frequency range of interest. 24 microphones type 40DB from the company G.R.A.S. are staggered and flush mounted at the outer casing downstream of the LP turbine. All the microphones are fully circumferentially movable. This type of microphone with sphere characteristic (sensitivity is the same in all spatial directions) is a ¼-inch prepolarized pressure microphone with a dynamic range upper limit of 170 dB and a frequency response from 10 Hz to 25 kHz (±1 dB). The preamplifier type 26AC has a very low inherent noise level as well as a dynamic range and a frequency response from below 2 Hz to 200 kHz (±0.2 dB). The first 12 microphones are placed in the non-cylindrical part of the flow duct with an axial displacement of 6 mm with respect to the center of the microphones. The acoustic measurement data out of this region will be used in the future in combination with an advanced mode analysis technique extended to non-cylindrical ducts. For the moment, since the established acoustic post processing tools are developed for flows in annular but cylindrical ducts (as e.g. described in Enghardt et al. (2001), Moser et al. (2009), Tapken and Enghardt (2006), Taddei et al. (2009)), it was important to maximize the number of microphones in the straight part of the measurement section (Figure 3). The results presented in this paper are taken from this downstream located microphone array II as post processing tools are only available for cylindrical ducts. Outcome of the optimization procedure was an axial distance between the microphones of 5 mm based on the investigations of Tapken and

Enghardt (2006) (see Figure 3). The first microphone of array I is located 177% of the LP blade chord length downstream of the blade trailing edge, the first microphone of array II at 434%.
For the data acquisition National Instruments equipment is used sampling the data with a frequency of 60 kHz. The post processing is done up to a frequency of 15 kHz. Additionally to the signal of the 24 microphones two shaft encoder systems are used to acquire a HP- and LP-trigger signal. The trigger signal was used to reconstruct the unsteady sound field by the rotor phases. The microphone array is traversed in steps of 2° and at each measurement point the signal from every channel is time-accurately acquired and stored during a data acquisition period of 20 seconds per measurement position. This corresponds to more than 1000 revolutions of the LP turbine and more than 3500 of the HP turbine. In total 180 measurement positions are recorded in one and a half hours.

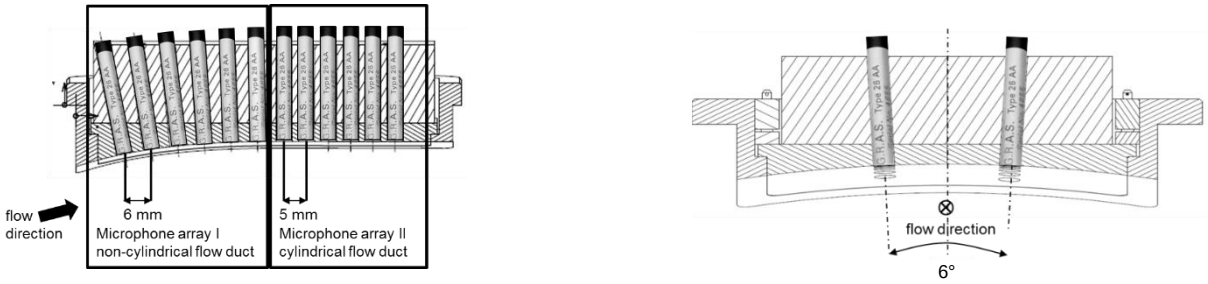

Figure 3: Meridional (left) and axis-orthogonal (right) views of the microphone arrays I and II

ACOUSTIC ANALYSIS

Since the two rotors of the test rig are counter-rotating and their rotational speeds are uncorrelated, the acoustic fields related to the HP-rotor and the LP-rotor, respectively, are analyzed separately. Therefore, phase averaging (Sharma et al. (1985), Suder et al. (1987), Hussain and Reynolds (1970)) and adaptive resampling (Lengani et al. 2012) are performed on the measured sound pressure. After a classical Fast Fourier Transformation (FFT) determining the harmonic frequencies induced by each rotor, the processed sound pressure can be described in terms of acoustic cut-on modes propagating in the duct at a specific frequency. These modes exhibit a certain circumferential pattern (detected by the Azimuthal Mode Analysis (Enghardt et al. 1999, Sijtsma and Zillmann 2007)), as well as radial pattern (detected by the Radial Mode Analysis (Tapken and Enghardt 2006, Sutliff 2005)) depending on the cut-on frequencies.

Phase Averaging, Adaptive Resampling and Modes of Interaction

In order to determine the acoustic effects induced by each rotor separately, a phase locked averaging based on the phase of one of the two rotors is done. Every revolution detected by the shaft encoders is split up to a fixed number of samples, thereby correcting the small speed variations of the two turbine shafts. The average of the samples at the same phase form the phase averaged values. Depending on the trigger used, the fluctuations of the flow quantities induced by the other rotor are then completely removed. This means that acoustic information generated by the HP rotor is removed when using the LP trigger and vice versa.
Sound pressure fluctuations at any circumferential position can be described as a sum of harmonics, represented by a Fourier series. For a cylindrical or annular duct solving the linearized wave equation leads to the space and time dependent sound pressure, which can be described in terms of acoustic modes. In order to allocate specific propagating modes to rotor-stator interactions in turbomachines, Tyler and Sofrin (1969) composed the following expression

$$m = hB \pm kV \tag{1}$$

where h is the harmonic index (1 for the 1st BPF, 2 for the 2nd BPF, etc.), B is the number of rotor blades, V is the number of stator vanes and the integer $k = \ldots, -1, 0, 1, \ldots$. It is possible to consider the interactions of the rotor with subsequent stages by simply superimposing the effect of the single event. For example, in a turbine a mode m* generated by a stator-rotor interaction will be scattered in the modes $m = m^* + k \cdot V_2$ with $k = \ldots, -1, 0, 1, \ldots$ by the following stator rows. Hence, for a stator-rotor-stator assembly the following modes are predicted:

$$m = hB + k_1 V_1 + k_2 V_2 \text{ with integers } k_1, k_2 \qquad (2)$$

V_1 and V_2 are the number of vanes of the first and second stator row, respectively.
Table 2 gives an overview over the propagating modes for the blade passing frequencies of each rotor depending on the corresponding swirl. It has to be noted that the cut-on mode regions show a slight asymmetric behavior due to the impact of the swirl. In the following, the azimuthal modes are presented and compared for the three different setups. The main modes, as explained in the following, are scattered by 8, which is a result of the linear combination of the different vane and blade counts of the two stages.

Table 2: Cut-on range and swirl for the BPF of the LP and of the HP rotor

	cut-on range	swirl
BPF_{HP}	-46,..,-44 : 8 : 36,..,45	13
BPF_{LP}	-29,..,-24 : 8 : 24,..,28	13

For the swirl, the model for rigid body swirl was used according to the following equation (with circumferential velocity c_u close to the outer endwall and the corresponding channel radius r):

$$\Omega = c_u / r \qquad (3)$$

The possible vane-blade interactions for both the LP as well as the HP stage are shown in Table 3 in terms of modes according to Eq. (1) and (2).

Table 3: Cut-on modes representing stator-rotor interactions at BPF_{HP} (a-c) and BPF_{LP} (d-e)

Interaction	Modes resulting from equations (1) and (2)										
(a) HP stator-HP rotor		-36;			-12;			+12;			+36;
(b) HP rotor-TMTF	-44;		-28;		-12;		+4;		+20;		+36;
(c) HP stator-HP rotor-TMTF	-44;	-36;	-28;	-20;	-12;	-4;	+4;	+12;	+20;	+28;	+36;	+44;
(d) HP stator-LP rotor	-24;			0;			+24;				
(e) TMTF-LP rotor	-24;		-8;		+8;		+24;				
(f) HP stator-TMTF-LP rotor	-24;	-16;	-8;	0;	+8;	+16;	+24;				

Azimuthal Mode Analysis (AMA)

The solution of the linearized wave equation for cylindrical ducts leads to the following expression for the space and time dependent sound pressure (Munjal (1997)):

$$p(x, r, \varphi, t) = \sum_{m=-\infty}^{\infty} \sum_{n=0}^{\infty} \left(A_{mn}^{+} e^{ik_{mn}^{+} x} + A_{mn}^{-} e^{ik_{mn}^{-} x} \right) \cdot f_{mn}\left(\sigma_{mn} \frac{r}{R}\right) e^{im\varphi} e^{-i\omega t} \qquad (4)$$

A_{mn}^{+} and A_{mn}^{-} are the complex amplitudes, k_{mn}^{+} and k_{mn}^{-} the axial wave numbers, downstream and upstream, respectively, m is the azimuthal mode order, n is the radial mode order, ω is the angular frequency, φ the circumferential position and R is the outer radius of the duct. The modal shape factor f_{mn}, depending on the hub-to-tip ratio r/R and the eigenvalues σ_{mn} of the specific geometry, represents the solution of the Bessel differential equation, describing the radial acoustic field considering hard wall boundary conditions (Tapken and Enghardt (2006), Sutliff (2005)).
In Eq. (5) A_m defines the complex azimuthal mode amplitudes at a specific frequency for each azimuthal mode order m (Sijtsma and Zillmann (2007)). These amplitudes are given as results of the AMA and are presented in the following section.

$$A_m(x,r)_f = \frac{1}{N_\varphi}\sum_{k=1}^{N_\varphi} p(x,r,\varphi_k)_f \, e^{-im\varphi_k} \tag{5}$$

RESULTS AND DISCUSSION

In the following, the setup with the larger tip gap and without any steps in the flow path is referred to as Basic Setup. It is compared to the setup, where the duct was laterally shifted (Shifted Setup), and the setup with the smaller tip gap.

Basic vs. Shifted Setup

Figure 4 shows the logarithmically summed up sound pressure comparing Basic and Shifted Setup. For the left part of the figure, the HP trigger was used and for the right one the LP trigger. It is important that for the calculation of these values just the cut-on modes were taken and as one can clearly see, no difference between the two setups can be found when using the HP trigger signal. With the LP trigger, the difference accounts for about 3 dB. In order to get a deeper insight into the noise generating mechanisms, the results of a FFT and of the azimuthal mode analysis are presented in the following figures. Again, two different trigger signals were applied for the data post processing.

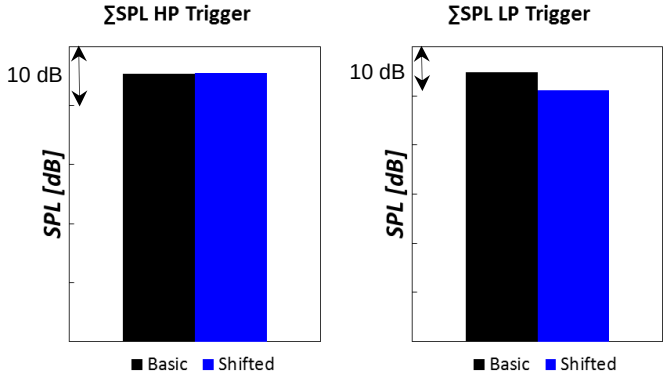

Figure 4: Summed up sound pressure levels for Basic and Shifted Setup; post processing using HP trigger on the left side and using LP trigger on the right side

HP Trigger

The left side of Figure 5 shows the spectrum for Basic and Shifted Setup after using the HP trigger for the averaging procedure. Therefore, the peaks corresponding to the blade passing frequency (BPF) of the HP rotor and its harmonics are dominating the spectrum. These frequencies are originating from the rotating blades passing a stationary observer and are therefore calculated from the number of blades and the rotational speed of the rotor. In order to make the figure clearer, the spectrum of the Shifted Setup was shifted by 100 Hz to the right. In the spectrum, no differences between the two setups can be seen, especially when regarding the tonal noise. The amplitudes of the peaks at the first and second BPF are the same and even the broadband noise does not differ. In this case, broadband noise due to stochastic fluctuations was completely removed due to phase averaging, which gets even clearer when regarding a FFT of the raw data (not shown here), where the broadband level is significantly higher as the stochastic parts of the signal are still included. Therefore, the parts of the

FFT named broadband noise have their origin in periodic parts of the signal. In Figure 5 for example, all the peaks, which do not correspond to the BPF of the HP rotor or to its harmonics originates from blade trailing edge shocks. After the FFT, an azimuthal mode analysis at the first BPF was carried out for the propagating modes in order to get a better understanding of the composition of the emitted tonal noise. The interactions that lead to the propagating modes in Figure 5 are given in Table 3. Although it is not shown here, it has to be mentioned that using the HP trigger, the amplitudes of the cut-off modes are significantly smaller than the amplitudes of the modes, which are cut-on. This is the reason, why the results of the AMA are in good accordance with the peak at the first BPF. There are no modes outside of the cut-on range with high amplitudes, which can have a significant influence on the peak in the spectrum as the spectrum also includes the cut-off modes. In the AMA, it is very hard to determine a certain pattern, whether some interactions are influenced more by the steps in the flow path than others. For most of the modes, the difference between the two setups is marginal and lies within the measurement uncertainty (±1dB).The amplitude of the two most dominant modes $m = -20$ and $m = -12$, is about the same for both test configurations. Due to the logarithmic summation of the mode amplitudes, which lead to the peak at the first BPF in the spectrum, just the most dominant peaks really influence the result. If the difference between two peaks at different modes is larger than 10 dB, the smaller peak can be neglected, as it does not influence the result. This is the reason why the spectrum shows the same amplitudes for both the Basic and the Shifted duct as the two most dominant modes have the same amplitude.

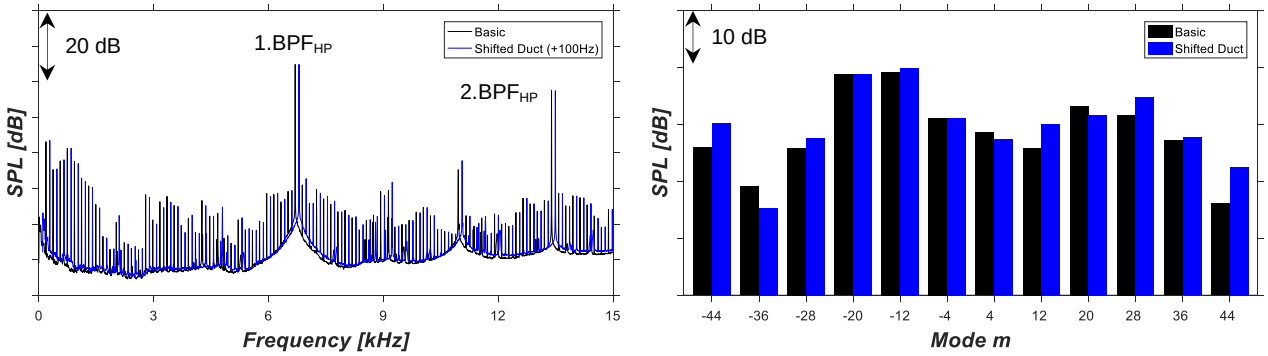

Figure 5: FFT comparing Basic and Shifted Setup (left side) and azimuthal mode analysis of the cut-on modes at 1.BPF$_{HP}$ (right side); both using the HP trigger

LP Trigger

Regarding the results after applying the LP trigger (see Figure 6), the situation is a bit different. For the first BPF of the LP rotor a significant difference between Basic and Shifted duct of about 5 dB can be seen. Interestingly, the steps in the flow path lead to a decrease in tonal noise emissions, which is also visible at the second BPF of the LP rotor, whereas the broadband noise level is the same as for the Basic setup. These deviations when using the LP trigger lead to the assumption that backward and forward facing steps in the flow path just have an impact on effects, which are correlated with the rotational speed of the LP rotor. At about 7 kHz there is a peak, which is not caused by the LP but by the HP rotor and corresponds to the first BPF. Even after using the LP trigger, periodic parts originating from the HP rotor can be detected. As the effects originating from the HP stage are very dominant (shocks emanated from the rotor and stator trailing edge), this peak is still visible even if it is not representative. The azimuthal mode analysis shows the propagating modes, which are cut-on, and especially the mode $m = -16$ shows a significant decrease in sound pressure level of about 13 dB for the Shifted duct. This mode originates from an interaction between HP stator, TMTF and LP rotor. Interestingly, the HP rotor is not involved. The same is valid for $m = -8$, which is either caused by an interaction between HP stator, TMTF and LP rotor or just TMTF and LP rotor At this mode a decrease of about 5 dB can be determined for the Shifted Setup.

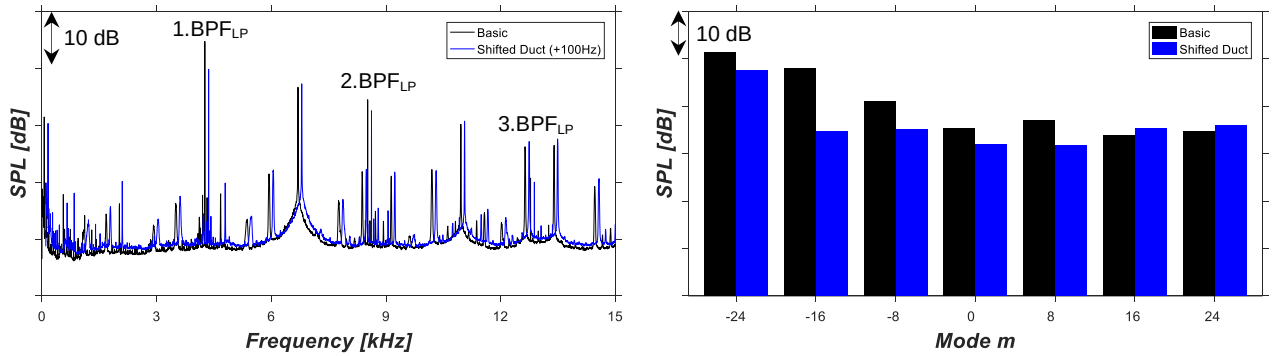

Figure 6: FFT comparing Basic and Shifted Setup (left side) and azimuthal mode analysis of the cut-on modes at 1.BPF$_{LP}$ (right side); both using the LP trigger

Two effects could cause a decrease in SPL when introducing backward and forward facing steps in the flow path. The first one is that the steps in the flow path can be compared to a reflective silencer, where sharp changes of the cross section lead to a reflection of acoustic waves and therefore to a noise reduction at the exit of the silencer. Shifting the duct laterally leads to a reflection of pressure waves at the hub and the tip and can therefore result in a reduced SPL further downstream of the steps. The impact of these reflections on the overall sound pressure level may be not too big, but nevertheless this effect should definitely be kept in mind. The second reason why the sound pressure level is reduced when shifting the duct could be explained with the theory of acoustic waves propagating in a horn. The acoustics in a channel with continuously changing cross section are described by a differential equation called Webster horn equation. The solution is given in Eq. (6):

$$p(x,\omega,t) = p_0 \cdot e^{\left(-\frac{\alpha}{2} \pm ik\sqrt{1-\frac{\alpha^2}{4k^2}}\right)\cdot x} \cdot e^{i\omega t} \qquad (6)$$

With the wave number k, the axial coordinate x and the constant α defining the opening angle of the horn. Based on principal investigations on forward facing steps, the scheme on the left side of Figure 7 was created for the situation in the currently regarded test rig. The steps cause a thicker boundary layer or even a separation bubble downstream of the interface between HP rotor casing and TMTF. This leads to a reduction of the effective flow area A_{eff} and works like a reduction of the duct radius at the TMTF inlet as the air is prevented from unobstructed flowing. To get an idea of the effect on the sound pressure, horn dimensions were calculated using the radii and axial distances of the duct (see middle plot of Figure 7). For the shifted duct, the effective channel radius at the channel inlet was just reduced by the step height plus 1 mm, which results in the significantly reduced pressure amplitude in Figure 7 (right picture) and a decrease in sound pressure level in Pascal corresponding to more than 2 dB. The step at the hub and a probable larger region with low momentum fluid at the endwalls, which further reduces the effective duct radius, were not even considered.

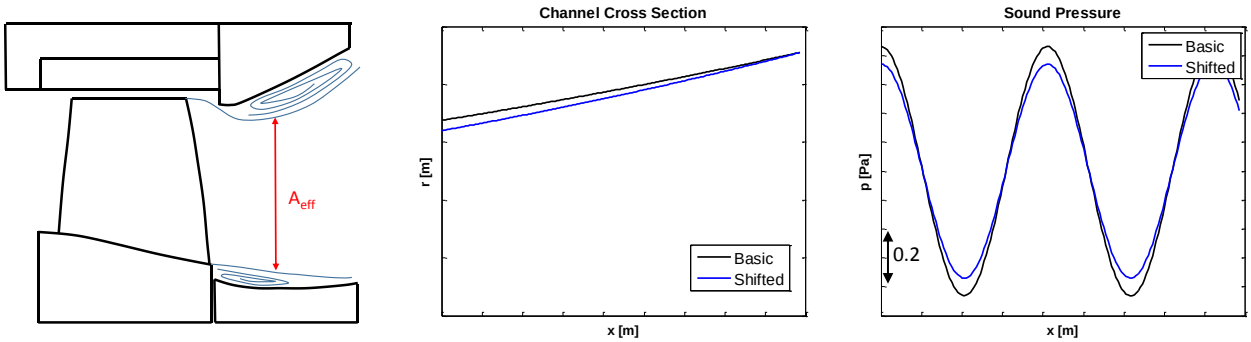

Figure 7: Schematic demonstration of different inlet radii of a horn on the sound pressure amplitude at a certain time step according to Webster's horn equation

Basic vs. Smaller Tip Gap

For the comparison between the Basic Setup and the setup with a smaller tip clearance, the same types of figures are presented as in the foregoing section. This time, neither the overall SPL using the HP trigger nor the overall SPL using the LP trigger reveals differences between the two setups. Again, the spectrum as well as the azimuthal mode analysis are supposed to give a deeper insight into the acoustics. Both are evaluated using the HP as well as the LP trigger signal.

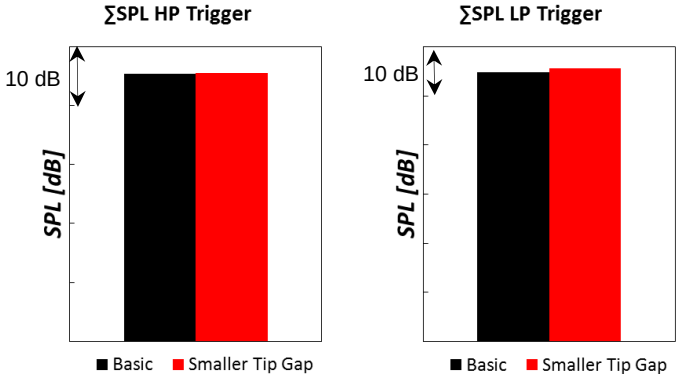

Figure 8: Summed up SPL for Basic and Smaller Tip Gap; post processing using HP trigger on the left side and using LP trigger on the right side

HP Trigger

When using the HP trigger in the post processing procedure, no difference can be seen between the two setups as expected from the plot of the overall sound power level. To get a deeper insight into the composition of the tonal noise at the first BPF of the HP rotor, the azimuthal mode analysis is shown for the cut-on modes (see right side of Figure 9).

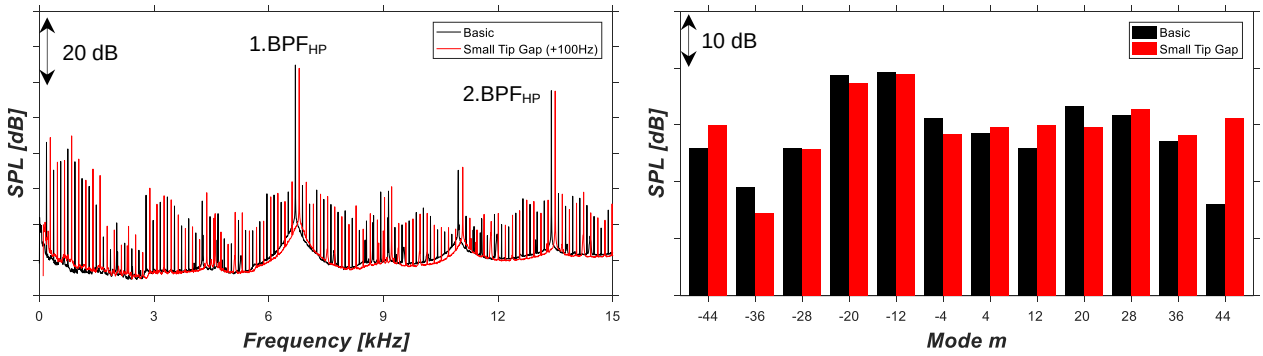

Figure 9: FFT comparing Basic and Smaller Tip Gap (left side) and azimuthal mode analysis of the cut-on modes at 1.BPF$_{HP}$ (right side); both using the HP trigger

For many modes, the difference lies within ±1 dB and is therefore negligible. Of course, there are modes where the difference is not negligible anymore e.g. $m = -36$ or $m = 44$, and which have their origin either in an interaction of HP stator-HP rotor-TMTF or HP rotor-TMTF. But as already mentioned, the amplitude at these modes is small compared to other modes (e.g. $m = -20$) and their influence on the overall SPL is therefore either small or can even be neglected, which results in very similar peaks at the first BPF for both test setups.

LP Trigger

Using the LP trigger, larger deviations between the setup with the larger and the setup with the smaller tip gap are depicted at the first BPF of the LP rotor. The tonal noise of the Basic Setup is approximately 2 dB higher than the noise of the setup with the smaller tip gap. When regarding the

AMA, the largest decrease in amplitude for the smaller clearance size can be seen at mode $m = -16$, which can just originate from an interaction of HP stator, TMTF and LP rotor. Although the geometrical changes are just related to the HP rotor, the most affected mode -16 is not related to an interaction with the HP rotor. This leads to the assumption that somehow a pressure pattern coming from the HP stator and interacting with the TMTF and the LP rotor further downstream, is changed or influenced by the reduced gap size. As the change in tip gap size can have an influence on many different parameters, which are related to acoustical characteristics like e.g. changed diffraction due to different tip gaps, it is very hard to determine the real cause for the amplitude differences.
Both Zhu and Carolus (2013) as well as Kameier and Neise (1997) found a significantly decreased broadband level when decreasing the tip clearance. For the fans they investigated, the difference accounted for up to 10 dB. In the turbine stage, which was investigated in this paper, the broadband levels did not differ that much. Regarding the spectrum in Figure 10, the maximum offset is 2 dB, especially at higher frequencies. However, the peaks at the blade passing frequencies of a turbine are more pronounced and significantly higher than the broadband noise. For the compressor fans presented by Zhu and Carolus and Kameier and Neise the difference between tonal and broadband noise is significantly smaller. This contrast between turbine and compressor stages is in good accordance with literature (see Bräunling (2009)).

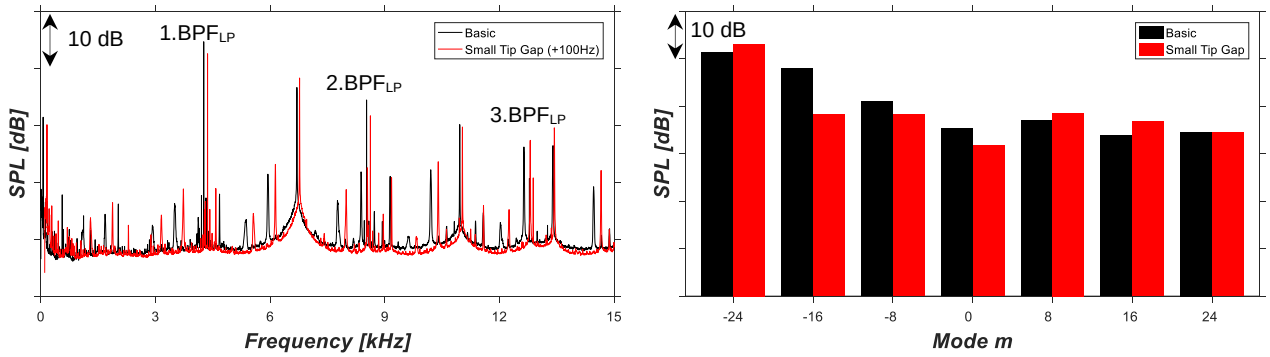

Figure 10: FFT comparing Basic and Smaller Tip Gap (left side) and azimuthal mode analysis of the cut-on modes at 1.BPF$_{LP}$ (right side); both using the LP trigger

CONCLUSIONS

In the currently presented paper, the influence of operational geometry changes on turbine acoustics was experimentally investigated using a microphone array downstream of a LP turbine. Operational changes are on the one hand steps in the flow path due to non-uniform warming of the parts and on the other hand changing tip clearance sizes. These effects occur particularly during the run-up and shut down of an engine and therefore, it is of big interest whether the noise emissions are influenced in a bad way, as this has become a very important issue for airports and airlines in the last few years. Fortunately, the investigations showed that neither steps in the flow path nor a smaller tip gap increase the noise emissions of the turbine. The shifting of the duct in order to generate the steps even lead to a SPL reduction of about 5 dB at the first BPF of the LP rotor. While the aerodynamics are usually influenced in a bad way by steps in the flow path, the acoustics obviously benefit as a clear reduction of sound emissions could be observed. Concerning the overall SPL, a reduction of 3 dB could be achieved with the laterally shifted setup using the LP trigger.
The smaller tip clearance resulted in a reduction of about 2 dB at the first BPF of the LP rotor, whereas no difference between the basic setup and the setup with smaller tip gap could be determined when calculating the overall sound pressure level.

ACKNOWLEDGEMENTS

The authors would like to thank Mr. H.P. Pirker as well as MTU Aero Engines, and Ulf Tapken from the DLR Institute of Propulsion Technology, Engine Acoustic Department.

REFERENCES

Bräunling, W. J. G. (2009). *Flugzeugtriebwerke.* Springer Verlag.

Enghardt, L., Tapken, U., Neise, W., Kennepohl F., Heinig K. (2001). *Turbine blade/vane interaction noise: acoustic mode analysis using in-duct sensor rakes*. 7th AIAA/CEAS Aeroacoustic Conference.

Enghardt, L., Zhang, Y., Neise, W. (1999). *Experimental Verification of a Radial Mode Analysis Technique using Wall-Flush Mounted Sensors*. Journal of The Acoustical Society of America, Vol. 105, 2.

Faustmann, C., Lengani, D., Spataro, R., Marn, A., Göttlich, E., Heimeir, F. (2013). *Experimental investigation of the noise generation and propagation for different turning mid turbine frame setups in a two-stage two-spool test turbine*. ASME Turbo Expo, Paper-No. GT2013-95698.

Faustmann, C., Zerobin, S., Marn, A., Spitalny, M., Broszat, D., Göttlich, E. (2014). *Noise generation and propagation for different turning mid turbine frame setups in a two shaft test turbine*. 20th AIAA/CEAS Aeroacoustic Conference, Paper-No. 1888811.

Hussain, A., Reynolds, W. (1970). *The meachanics of an organized wave in turbulent shear flow*. Journal of Fluid Mechanics, Vol. 41, 241-258.

Kameier, F., Neise, W. (1997). *Experimental Study of Tip Clearance Losses and Noise in Axial Turbomachines and Their Reduction.* Journal of Turbomachinery, Vol. 119, pp. 460-471.

Lengani, D., Santner, C., Spataro, R., Göttlich, E. (2012). *Analysis tools for unsteady interactions in a counter-rotating two-spool turbine rig*. Experimental Thermal Fluid Science, Vol. 42, pp.248-257.

Moser, M., Tapken, U., Enghardt, L., Neuhaus, L. (2009). *An Investigation of LP-Turbine blade/-vane interaction noise: Measurements in a 1.5 stage rig*. Journal of Power and Energy, Vol. 223, No. 6, pp 687-695.

Munjal, M. L. (1997). *Acoustic of Ducts and Mufflers.* New York : John Wiley & Sons.

Santner, C., Paradiso, B., Malzacher, F., Hoeger, M., Hubinka, J., Göttlich, E. (2011). *Evolution of the flow through a turning mid turbine frame applied between a transonic HP-Turbine stage and a counter-rotating LP-Turbine*. 9th European Turbomachinery Conference.

Sharma, O. P., Butler, T. L., Joslyn, H., D., Dring, R., P. (1985). *Three-dimensional unsteady flow in an axial flow turbine*. AIAA Journal of Propulsion and Power, 1 (1), pp. 29-38.

Sijtsma, P., Zillmann, J. (2007). *In-duct and farfield mode detection techniques*. 13th AIAA/CEAS Aeroacoustic Conference.

Suder K.L., Hathaway M.D., Okiishi T.H., Strazisar A.J., Adamczyk J.J. (1987). *Measurements of the unsteady flow field within the stator row of a transonic axial-flow fan: Part 1-Measurement and analysis technique*. NASA Technical Memorandum 88945.

Sutliff, D. L. (2005). *Rotating Rake Turbofan Duct Mode Measurement System*. NASA Technical Memorandum 213828.

Taddei, F., De Lucia, M., Cinelli, C., Schipani, C. (2009). *Experimental investigation of low pressure turbine noise: radial mode analysis for swirling flows*. ISUAAAT12, Paper-No. I12-S4-4.

Tapken, U., Enghardt, L. (2006). *Optimization of Sensor Arrays for Radial Mode Analysis in Flow Ducts*. 12th AIAA/CAES Aeroacoustics Conference.

Tyler, J. M., Sofrin, T. (1969). *Axial flow compressor noise*. SAE Transaction 70, pp. 309-332.

Zhu, T., Carolus, T. (2013). *Experimental and unsteady numerical investigation of the tip clearance noise of an axial fan.* ASME Turbine Blade Tip Symposium and Course Week, Paper No. TBTS2013-2034.